1st International Workshop on Geoelectrical Monitoring, GELMON 2011, VIENNA, 30.11.2011-2.12.2011

Comparison of temperature estimates from heat transport model and electric resistivity tomography during a shallow heat injection and storage experiment

T. Hermans[1,2], M. Daoudi[1], A. Vandenbohede[3], T. Robert[1], D. Caterina[1,2], F. Nguyen[1]

[1]University of Liège, Belgium, ArGEnCo, GEO³, Applied Geophysics
[2]F.R.S.-FNRS, Belgium
[3]Ghent University, Belgium, Department of Geology and Soil Science, Research Unit Groundwater Modeling

Abstract

Groundwater resources are increasingly used around the world as geothermal systems. Understanding physical processes and quantification of parameters determining heat transport in porous media is therefore important. Geophysical methods may be useful in order to yield additional information with greater coverage than conventional wells. We report a heat transport study during a shallow heat injection and storage field test. Heated water (about 50°C) was injected for 6 days at the rate of 80 l/h in a 10.5°C aquifer. Since bulk electric resistivity variations can bring important information on temperature changes in aquifers (water electric conductivity increases about 2%/°C around 25°C), we monitored the test with surface electric resistivity tomography and demonstrate its ability to monitor spatially temperature variations. Time-lapse electric images clearly show the decrease and then the increase in bulk electric resistivity of the plume of heated water, during respectively the injection and the storage phase. This information enabled to calibrate the conceptual flow and heat model used to simulate the test. Inverted resistivity values are validated with borehole electromagnetic measurements (EM39) and are in agreement with the temperature logs used to calibrate the parameters of the thermo-hydrogeological model for the injection phase. The short term evolution of the ERT-derived temperature and the temperature logs is coherent for both a qualitative and quantitative use of ERT-derived temperature. However, the mid- and long-term evolution need to account for other phenomena such as variations of TDS content as a function of temperature to quantitatively use ERT estimates as temperature proxy. This field work demonstrates that surface electric resistivity tomography can monitor heat injection and storage experiments in shallow aquifers. These results could potentially lead to a number of practical applications, such as the monitoring or the design of shallow geothermal systems or the use of heated water to replace salt water in tracer tests.

Keywords: electric resistivity tomography, thermal test, thermal properties, hydrogeological modeling, time-lapse monitoring.

Introduction

The production of geothermal energy is increasingly growing worldwide. Groundwater, through the use of geothermal heat pumps, accounts for a major part in the thermal energy use and installed capacity (Lund, 2010).

Geothermal energy does not rely only on high temperature and deep systems. Indeed, very low temperature systems (< 30°C) are much more easily accessible, relatively abundant in alluvial or coastal plains for example, involve lower implementation costs and may be used for cooling or heating (Allen and Milenic, 2003).

To design and exploit geothermal energy systems through pumping or storage of water, engineers must estimate the parameters governing heat transport processes. These are mainly heat capacity and thermal conductivity of fluid and solid. Engineers generally rely on standard calculation charts, which may not be representative of *in situ* conditions, such as the influence of the soil/rock, the well and the fluid, or on thermal response tests in wells, which deliver only well-centered information (similar to pumping tests). In this context, electric resistivity tomography (ERT) can bring relevant spatial and temporal information through the correlation between temperature and bulk electric resistivity changes with a greater coverage than single wells for *in situ* studies. In analogy to salt tracer tests regularly performed in the field of hydrogeophysics, one can monitor temperature variations of aquifers and exploit their effect on electric conductivity (Ptak et al., 2004; Hermans et al., 2012).

In this paper, we extended the work of Vandenbohede et al. (2011) and Hermans et al. (2012) who monitored a heated water injection test with ERT and showed that ERT-derived temperatures could reproduce qualitatively and quantitatively temperatures obtained with a calibrated thermo-hydrogeological model. However, in this first test, only the injection phase was monitored. Here, we look at the possibility of monitoring the storage phase with ERT. Heated water (about 50°C) was injected for 6 days at the rate of 80 l/h in a 10.5°C aquifer and the storage phase was monitored for ten days.

First, we will review the site-specific petrophysical relationships and briefly present the study site. Then, the results of the injection test will be presented. After that, we will present the results of the storage phase and highlight the challenges associated with it. Finally, we will draw conclusions.

Petrophysics

In the range of temperature considered in this test (10 to 50°C), a linear dependence between water electric conductivity and temperature can be assumed (Hayley et al., 2007; Hermans et al., 2012)

$$\frac{\sigma_T}{\sigma_{25}} = m(T - 25) + 1 \tag{1}$$

where σ_T is the water electric conductivity at temperature T (in °C) and m is the fractional change in electric conductivity per degree Celsius. The value of m can be experimentally determined and is equal to 0.02125 in this specific case (Hermans et al., 2012).

A similar relationship can be used to model surface conductivity. However, in our case, the experiment took place in a sandy aquifer free of clays. Even if silica grains have a surface conductivity, it is in our case three orders of magnitude below water electric conductivity and was thus neglected (Revil and Linde, 2006 ; Hermans et al., 2012).

Using Archie's law, the link between bulk electric conductivity and temperature is therefore straightforward. Indeed, if surface conductivity is neglected, the ratio of Archie's law between two time-steps enables to deduce the water electric conductivity ratio

$$\frac{\sigma_{b2}}{\sigma_{b1}} = \frac{\sigma_{w2}}{\sigma_{w1}} \quad (2)$$

where σ_b is the bulk electric conductivity and σ_w is the water electric conductivity. In equation 2, σ_{b1}, σ_{b2} and σ_{w1} are known from ERT measurements for the first two parameters and from well water samples for the latest. Finally, using equation 1, the temperature of water can be easily deduced.

Study site

The field experiments took place on the campus De Sterre of Ghent University, Belgium. The subsurface is composed of two layers. The upper layer lies from 0 to -4.4 m and corresponds to homogeneous Quaternary fine sands. From -2 m down to -4.4 m, these sands are found at saturation. Below -4.4 m, a clay layer of Tertiary age is found, forming a low permeability layer. The injecting well was drilled down to -4.4 m; it is made of a PVC casing with a screen of 90 cm at the bottom of the Quaternary layer. The temperature in the aquifer was 10.5°C.

Injection phase (Hermans et al., 2012)

A first test was done in February 2010 to monitor the injection during 3 days of heated water (48°C) into the 10.5°C aquifer. During this test, tap water was used for injection. However, tap water and formation water do not have the same electric conductivity, which are 374 and 676 µS/cm at 10.5°C respectively. Consequently, the increase in conductivity with temperature was partly counterbalanced by the lower conductivity of injection water.

An additional step was thus necessary to derive temperatures from ERT measurements. We had to calculate with a flow and transport model the water electric conductivity distribution resulting from the injection of less conductive water and to use the corresponding σ_{25} value in equation 1 instead of using the reference value from formation water (Hermans et al., 2012).

This process led to Fig. 1 where temperatures from calibrated modeling and ERT after 3 days of injection are compared. Temperatures monitored with ERT are quite consistent with the thermo-hydrogeological model after 72h. The maximum temperature deduced from ERT is 45°C which is only 3°C below the mean temperature of injection. The width and thickness of the plume are also satisfactory. The enlargement of the plume can be easily explained by the smoothness constraint used to regularize the model differences in the inversion process. Nevertheless, it is in part counterbalanced by the spatial distribution of the proportion of tap and formation water obtained from hydrogeological simulations. More details can be found in Hermans et al. (2012).

Storage phase

During the first test, the aim was to see if ERT measurements were able to predict temperatures in the aquifer. In a second attempt, we tried to extend the process to the storage phase of the experiment and to avoid the step of flow modeling to predict temperatures. Due to logistic constraints, it was not possible to inject formation water directly. So, we decided to inject cold tap water in the well during two weeks to have a bell of injected water around the well before the beginning of injection of heated water. This also enables a larger contrast in terms of electric conductivity. In addition, we extended the injection of heated water to 6 days. We used a dipole-dipole configuration with an electrode spacing of 60cm to reach the targeted depth of investigation (3 to 4.5m). Reciprocal measurements were taken for each time-step to assess the level noise and data were

weighted accordingly during the inversion. Specific considerations about the noise level were presented in Nguyen et al. (2011).

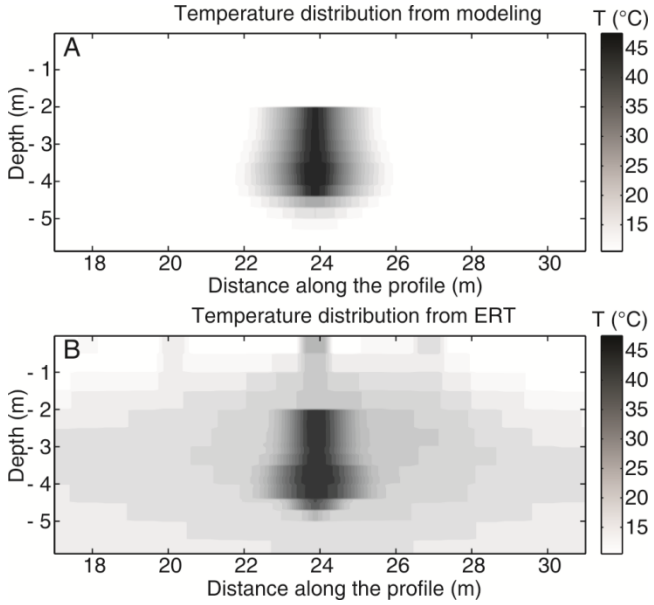

Figure 1. *Petrophysical laws enabled to transform resistivity values into temperatures. The plume detected after 3 days of injection with ERT (B) is in accordance with the plume calculated with a calibrated thermo-hydrogeological model (A) (Hermans et al., 2012).*

During the storage phase, ERT is able to highlight the decrease in temperature of injected water, which corresponds to a decrease in the resistivity anomaly. The decrease in resistivity is maximum at the end of injection; then, it tends progressively to zero. Fig. 2 shows this anomaly after 4 days (A) and 9 days (B) of cooling. At this time, a decrease in resistivity of -20% compared to the background is still visible. The plume is enlarged due to the smoothing effect of the regularization. In this case, the effect would be also visible in an ERT-derived temperature section (in contrast with Fig. 1), because the effect is not counterbalanced by the contrast of conductivity between formation and injection water. Note also the increase of resistivity in the upper part of the image, due to the desaturation of the unsaturated area which was almost saturated for the background due to a rainfall event.

We validated the obtained resistivity values with borehole measurements. We performed electromagnetic measurements in the well with an EM39 device to obtain a conductivity log (Fig. 3A). The results are very similar four days after the end of injection, which proves that ERT is a reliable tool to predict electric conductivity.

However, when we look at the correspondence with temperature logs (Fig. 3B and 3C), we see that the results are much worse than in Fig. 1. Since electric conductivity seems to be correctly resolved, we assume that the discrepancy results from the transformation of electric conductivity to temperatures. Fig. 2A is taken 10 days after the beginning of injection, compared to 3 days for Fig. 1. Some other phenomena may be responsible for a change in electric conductivity other than the temperature effect for mid- and long-term sections. These could be related to modifications of the TDS content related with absorption/desorption or dissolution/precipitation phenomena that are both affected by temperatures since most chemical constants are temperature dependent. An effect of diffusion between formation and injection water is also possible since a concentration gradient exists.

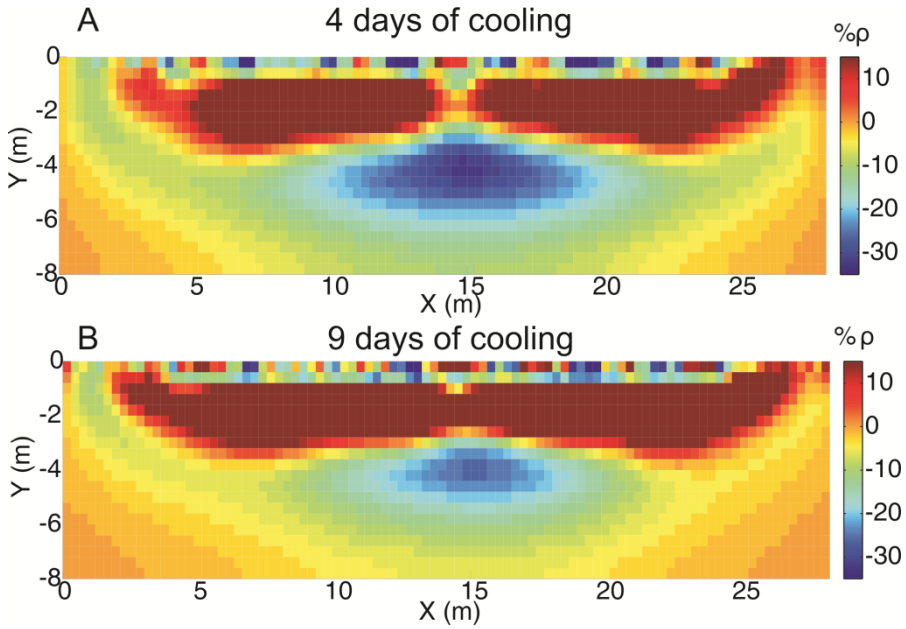

Figure 2*. ERT time-lapse images show, as expected, a decrease of the resistivity anomaly during the cooling phase between 4 (A) and 9 (B) days of cooling. In the upper part of the model, an increase in resistivity due to a change of saturation in the unsaturated zone related to changing weather conditions (for the background, the soil was almost saturated due to strong precipitations) is also visible.*

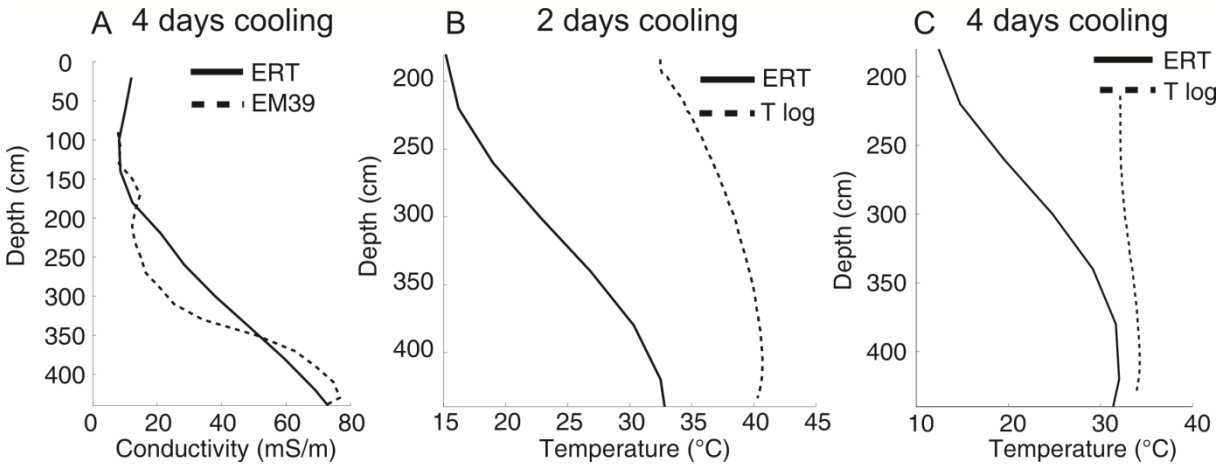

Figure 3*. ERT measurements were validated using EM39 measurements (A). In the zone of injection, ERT is really closed to EM39 data. Once transformed in temperatures, we observe a gap between ERT and temperatures logs after both 2 days (B) and 4 days of cooling (C). Since, this gap was not observed for the injection phase (Fig. 1), a more complex petrophysical relationship may be necessary to understand the phenomenon.*

Conclusion

This work demonstrates the ability of ERT to monitor qualitatively and quantitatively shallow geothermal tests. If the injection of tap water can be a drawback since it can reduce the measured contrast, combined with a flow and transport model, it enables to improve the estimation of temperatures in the aquifer. This injection scheme could be use in combination with traditional pumping and tracer tests to derive in a first step hydraulic conductivity and dispersivity, and in a

second step, thermal properties. Coupled inversions could also be developed to avoid the regularization step of ERT inversions.

If we consider an electrode spacing *a* of 60cm, we can deduce guidelines for further studies, since we imaged successfully a plume of heated water at a depth of 5*a*, a thickness of 4*a* and a width of 5*a* with a dipole-dipole configuration ($a = 3$ and $n \leq 13$).

Laboratory measurements must be performed to further study the complex effect of temperature on the electric conductivity of water for mid- and long-term experiments, including potential changes related to dissolution and absorption phenomena.

Our approach should in time contribute to the development of *in situ* techniques to characterize groundwater and porous matrix properties governing heat transfer in the subsurface and to monitor shallow geothermal resources exploitation. It could also contribute to the development of techniques of thermal tracers, when salt tracers are not allowed.

References

Allen, A. and D. Milenic, 2003, Low-enthalpy geothermal energy resources from groundwater in fluvioglacial gravels of buried valleys, Applied Energy, **74**, 9-19, doi: 10.1016/S0306-2619(02)00126-5.

Hayley, K., L.R. Bentley, M. Gharibi and M. Nightingale, 2007, Low temperature dependence of electrical resistivity: Implications for near surface geophysical monitoring, Geophysical research letters, **34**, L18402, doi: 10.1029/2007GL031124

Hermans, T., A. Vandenbohede, L. Lebbe and F. Nguyen, 2012, A shallow geothermal experiment in a sandy aquifer monitored using electric resistivity tomography, Geophysics, **77**(1), B11-B21, doi: 10.1190/GEO2011-0.199.1

Lund, J.W., 2010, Direct utilization of geothermal energy, Energies, **3**, 1443-1471, doi: 10.3390/en3081443.

Nguyen, F., A. Kemna, T. Robert, T. Hermans, D. Caterina and A. Flores-Orozco, 2011, Inversion of multi-temporal geoelectrical data sets: insights from several case studies, GELMON, 1st International Workshop on Geoelectrical Monitoring, Vienna, Austria, December 1.

Ptak, T., M. Piepenbrink and E. Martac, 2004, Tracer tests for the investigation of heterogeneous porous media and stochastic modeling of flow and transport-a review of some recent developments, Journal of Hydrology, **294**, 122-163, doi: 10.1016/j.jhydrol.2004.01.020.

Revil, A. and N. Linde, 2006, Chemico-electrochemical coupling in microporous media, Journal of colloid and interface science, **302**, 682-694, doi: 10.1016/j.jcis.2006.06.051.

Vandenbohede, A., T. Hermans, F. Nguyen and L. Lebbe, 2011, Shallow heat injection and storage experiment: heat transport simulation and sensitivity analysis, Journal of hydrology, **409**, 262-272, doi: 10.1016/j.jhydrol.2011.08.024.